Natural and anthropogenic radionuclide distributions in the Nansen Basin, Artic Ocean: Scavenging rates and circulation timescales

J. KIRK COCHRAN,* DAVID J. HIRSCHBERG,*
HUGH D. LIVINGSTON,† KEN O. BUESSELER† and
ROBERT M. KEY‡

Abstract—Determination of the naturally occurring radionuclides ^{232}Th, ^{230}Th, ^{228}Th and ^{210}Pb, and the anthropogenic radionuclides ^{241}Am, ^{239,240}Pu, ^{134}Cs and ^{137}Cs in water samples collected across the Nansen Basin from the Barents Sea slope to the Gakkel Ridge provides tracers with which to characterize both scavenging rates and circulation timescales in this portion of the Arctic Ocean. Large volume water samples (∼ 1500 l) were filtered *in situ* to separate particulate (> 0.5 μm) and dissolved Th isotopes and ^{241}Am. Thorium-230 displays increases in both particulate and dissolved activities with depth, with dissolved ^{230}Th greater and particulate ^{230}Th lower in the deep central Nansen Basin than at the Barents Sea slope. Dissolved ^{228}Th activities also are greater relative to ^{228}Ra, in the central basin. Residence times for Th relative to removal from solution onto particles are ∼ 1 year in surface water, ∼ 10 years in deep water adjacent to the Barents Sea slope, and ∼ 20 years in the Eurasian Basin Deep Water. Lead-210 in the central basin deep water also has a residence time of ∼ 20 years with respect to its removal from the water column. This texture of scavenging is reflected in distributions of the particle-reactive anthropogenic radionuclide ^{241}Am, which shows higher activities relative to Pu in the central Nansen Basin than at the Barents Sea slope.

Distributions of ^{137}Cs show more rapid mixing at the basin margins (Barents Sea slope in the south, Gakkel Ridge in the north) than in the basin interior. Cesium-137 is mixed throughout the water column adjacent to the Barents Sea slope and is present in low but detectable activities in the Eurasian Basin Deep Water in the central basin. At the time of sampling (1987) the surface water at all stations had been labeled with ^{134}Cs released in the 1986 accident at the Chernobyl nuclear power station. In the ∼ 1 year since the introduction of Chernobyl ^{134}Cs to the Nansen Basin, it had been mixed to depths of ∼ 800 m at the Barents Sea Slope and to ∼ 300 m in the central basin. "Pre-Chernobyl" inventories of ^{137}Cs (as well as ^{239,240}Pu) are 10 times those expected from global atmospheric fallout from nuclear weapons testing and are derived principally from releases from the Sellafield, U.K., nuclear fuel reprocessing facility on the Irish Sea. Based on the sources of ^{137}Cs to the Nansen Basin, mixing time scales are 9–18 years for the upper water column (to 1500 m) and ∼ 40 years for the deep water. These mixing time scales, combined with more rapid scavenging at the basin margin relative to the central basin, produce residence times of particle-reactive radionuclides in the Nansen Basin comparable to other open ocean areas (e.g. north-west Atlantic) despite the presence of permanent ice cover and long periods of low-light levels that limit productivity in the Arctic.

* Marine Sciences Research Center, State University of New York, Stony Brook, NY 11794-5000, U.S.A.
† Department of Chemistry, Woods Hole Oceanographic Institution, Woods Hole, MA 02543, U.S.A.
‡ Program in Atmospheric and Oceanic Sciences, Princeton University, Princeton, NJ 08544, U.S.A.

INTRODUCTION

The suite of naturally-occurring and anthropogenically-produced radionuclides contains tracers suitable for studying transport of both particles and water in the oceans. Several of the radionuclides of the uranium and thorium decay series, in particular the Th isotopes ^{230}Th (half-life = 75,000 years) and ^{228}Th (half-life = 1.9 years) and the Pb isotope ^{210}Pb (half-life = 22 years), are produced in seawater from decay of dissolved precursors (^{234}U, ^{228}Ra and ^{226}Ra, respectively), become associated with particles, and are removed from the water column.

Deliberate and accidental releases of anthropogenic radionuclides to the oceans provide transient tracers that are also useful for studying scavenging and circulation processes (Kupferman *et al.*, 1979; Bowen *et al.*, 1980; Livingston *et al.*, 1982, 1984, 1985). The Pu isotopes and ^{241}Am can associate with particle surfaces, and their distributions in the oceans are affected by scavenging and particle transport. Americium-241 in particular has a chemical behavior comparable to Th in its particle reactivity (Fisher *et al.*, 1988; Cochran *et al.*, 1987). Cesium-137, on the other hand, exhibits only weak particle reactivity in the open ocean, and its distribution is largely controlled by advection and mixing of water. Dumping of spent nuclear fuel, reactor parts and radioactive waste in the Kara Sea by the former Soviet Union has led to recent interest in the chemical behavior and fate of anthropogenic radionuclides in the Arctic Ocean. In this context, the natural U and Th series radionuclides can be used to provide clues to the processes controlling the distributions of their anthropogenic counterparts because the source functions of the natural nuclides are well characterized and their distributions tend toward a steady state.

Within the last decade, significant insights into the texture of scavenging of chemical species in the oceans have been gained from distributions of particle-reactive radionuclides (Nozaki *et al.*, 1981; Bacon and Anderson, 1982; Mangini and Key, 1983; Bacon *et al.*, 1985; Bruland and Coale, 1986; Cochran *et al.*, 1987; Coale and Bruland, 1987; Huh and Beasley, 1987). Higher rates of particle production and flux in the surface ocean and at the ocean margins make these areas generally more effective scavenging regimes. Indeed transport of reactive radionuclides such as ^{210}Pb and ^{231}Pa to ocean margins followed by intense scavenging in these areas has been used to explain the distributions and gradients of these radionuclides away from the margins to the basin interior (Carpenter *et al.*, 1981; Anderson *et al.*, 1983a,b; Cochran *et al.*, 1983, 1990; Bacon, 1988).

The Arctic Ocean has been regarded as an environment of low scavenging intensity relative to other open ocean areas because the permanent ice cover and extended periods of darkness during the Arctic winter serve to inhibit particle production and sinking. This possibility was first raised by Ku and Broecker (1967) and Finkel *et al.* (1977) to explain low activities and inventories of ^{230}Th and ^{10}Be, respectively, in Arctic Ocean sediments. More recently, Moore and Smith (1986) and Bacon *et al.* (1989) have shown that scavenging of ^{210}Pb and Th isotopes is slower in the waters of the Canada Basin relative to the open oligotrophic ocean. We present here distributions of natural and anthropogenic radionuclides in the Nansen Basin and show that removal of particle-reactive radionuclides is more rapid in this basin than in the Canada Basin. The difference is likely due to more rapid ventilation of the Nansen Basin coupled with enhanced scavenging in the slope and broad marginal Arctic shelf.

Sampling and analytical methods

Water and sediment samples were collected during the 1987 ARK IV/3 cruise of the R.V. *Polarstern* (Fig. 1). Water samples for Th isotopes and [241]Am were taken by *in-situ* pumps which filter large volumes of water through 0.5 μm polypropylene wound fiber cartridge prefilters and two similar cartridges loaded with manganese oxide. The former retain the fine particulate fraction, while the latter adsorb dissolved thorium (Cochran *et al.*, 1987; Livingston and Cochran, 1987; Buesseler *et al.*, 1992). Two modifications to previous sampling procedures with the pumps (Cochran *et al.*, 1987) were made on the ARK IV/3 cruise. The manganese adsorber cartridges were not prepared in the laboratory before the cruise by soaking in hot $KMnO_4$ solution, but instead were loaded with freshly precipitated manganese oxide before each deployment. The MnO_2 was formed from a solution of $MnCO_3$ and $KMnO_4$ at pH = 8 and was filtered onto the cartridge. In addition, a few of the pump samples were taken with two prefilter cartridges in series, followed by the two manganese adsorber cartridges. The purpose of this modification was to check for possible artifacts caused by sorption of dissolved Th onto the prefilter cartridge.

The cartridges were returned to the laboratory where they were dried and ashed at 450°C. The ash was dissolved in HNO_3 in the presence of [229]Th and [243]Am yield tracers. Thorium
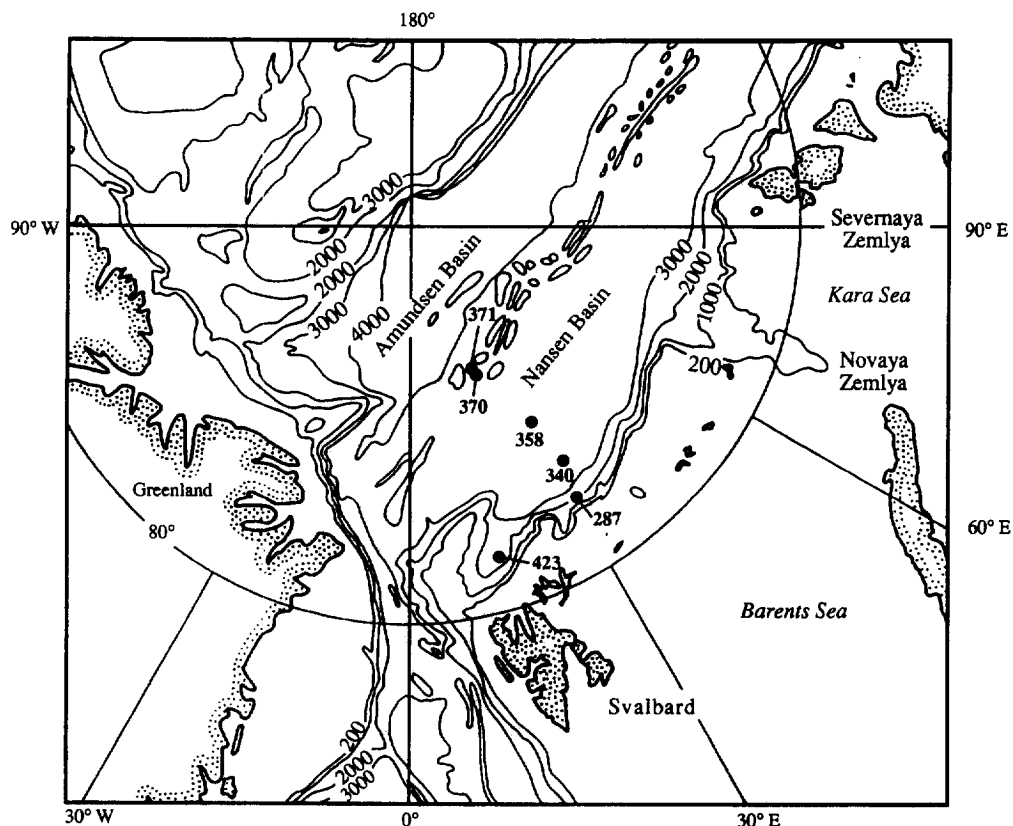

Fig. 1.   Map of the Nansen Basin showing stations sampling for radionuclides during cruise ARK IV/3 of the R.V. *Polarstern*.

was separated from Am by ion exchange. The Am and Th fractions were further purified by ion exchange and subsequently electrodeposited for alpha spectrometry (Cochran *et al.*, 1987). Prefilters and cartridges deployed in pumps that failed to operate were used as blanks.

Water samples also were taken by hydrocast (Gerard barrels) for analysis of ^{239,240}Pu, ^{134,137}Cs and ^{90}Sr (Livingston *et al.*, 1975). These samples were acidified to pH 2, stored in 60 l delex containers and returned to the laboratory for processing. Aliqots (4 l) from two stations were taken from the 60 l samples for ^{210}Pb analysis. Polonium-209 tracer and Fe carrier were added to these samples and iron hydroxide was precipitated. Lead-210 was determined by plating and counting its ^{210}Po daughter (Flynn, 1968). Because the samples were processed and analyzed 1.5 years after collection, ^{210}Po should be within about 5% of equilibrium with ^{210}Pb.

Samples for Ra isotopes were collected from large volume (300 l) samples taken for radiocarbon. After the ^{14}C had been converted to CO_2 by acidification and stripped from the samples, the pH was adjusted to 7 and radium was extracted by passing the sample through acrylic fiber coated with MnO_2 (Moore, 1976; Moore *et al.*, 1985). The ^{228}Ra/^{226}Ra activity ratio was measured on these samples. Because this procedure does not result in quantitative removal of Ra from solution, small volume (20 l) samples are generally taken for independent determination of ^{226}Ra. This was not done on the ARK IV/3 cruise, and as a consequence only ^{228}Ra/^{226}Ra ratio data are available for those samples. The ^{228}Ra/^{226}Ra data are reported in detail by Rutgers van der Loeff *et al.* (1995).

RESULTS

The thorium isotope data are presented in Table 1. Extraction efficiencies for each Mn cartridge pair were calculated from

$$\text{Efficiency} = 1 - \text{Mn}B/\text{Mn}A \qquad (1)$$

where MnB is the activity on the second cartridge and MnA is the activity on the first cartridge.

Efficiencies generally ranged between 65 and 100% (based on ^{230}Th activities) with a mean ± 1 s.d. of 74.0 $\pm$ 17.0%. A few samples had values less than 50%, and the uncertainties in the resultant dissolved activities were large. These data have not been included in Table 1. The mean extraction efficiency with the cartridges loaded with pre-formed MnO_2 is lower than that for cartridges impregnated with MnO_2 by soaking in hot $KMnO_4$ (Cochran *et al.*, 1987; Buesseler *et al.*, 1992), and we conclude that the latter is a better procedure.

The blank contribution to sample peaks was generally less than 40% for ^{232}Th, 25% for ^{230}Th and 5% for ^{228}Th. Uncertainties reported in Table 1 were calculated from one sigma counting uncertainties propagated in the blank, sample activities and cartridge extraction efficiencies.

Some ^{228}Ra is extracted from seawater onto the Mn cartridges, and then dissolved ^{228}Th data must be corrected for ingrowth from ^{228}Ra between sample collection and initial separation of Th and Ra. As the first step in making this correction, we calculated ^{228}Ra activities from the measured ^{228}Ra/^{226}Ra activity ratios and ^{226}Ra activities calculated from dissolved Si data. The estimation of ^{226}Ra used the ^{226}Ra–Si relationship obtained from TTO Stas 142–162 (Key *et al.*, 1992). In effect these stations constitute the source water for

Table 1. Nansen Basin thorium isotope data

Depth (m)	Particulate (dpm/1000 l)			Dissolved (dpm/1000 l)			^{228}Ra (dpm/1000 l)
	^{232}Th	^{230}Th	^{228}Th	^{232}Th	^{230}Th	^{228}Th	
Sta. 287 (81°40'N, 30°48'E, 2250 m)							
6	0.0165 ± 0.0050	0.0125 ± 0.0089	0.357 ± 0.041	0.0382 ± 0.0062	0.0919 ± 0.0172	7.26 ± 3.26	20.9 ± 1.1
50	0.0060 ± 0.0060	0.0130 ± 0.0110	0.636 ± 0.071	0.0402 ± 0.0080	0.0626 ± 0.0141	7.28 ± 1.17	27.6 ± 1.6
350	0.0397 ± 0.0074	0.0298 ± 0.0123	0.917 ± 0.066	0.0156 ± 0.0074	0.0924 ± 0.0196	6.82 ± 0.69	18.9 ± 1.1
500	0.0493 ± 0.0060	0.0670 ± 0.0100	0.841 ± 0.053	0.0549 ± 0.0102	0.129 ± 0.023	5.04 ± 0.73	19.4 ± 1.2
1050	0.0514 ± 0.0052	0.102 ± 0.011	0.623 ± 0.036	0.0213 ± 0.0039	0.227 ± 0.021	2.80 ± 0.21	7.1 ± 0.5
1450	0.0901 ± 0.0083	0.238 ± 0.019	0.742 ± 0.038	0.0315 ± 0.0138	0.290 ± 0.048	2.92 ± 0.45	6.1 ± 0.6
2150	0.0999 ± 0.0064	0.254 ± 0.017	0.660 ± 0.026	0.0226 ± 0.0042	0.270 ± 0.026	1.77 ± 0.15	5.1 ± 0.7
Sta. 358 (84°00'N, 30°46'E, 4050 m)							
50	0.0039 ± 0.0027	0.0125 ± 0.0079	1.19 ± 0.06	0.0132 ± 0.0044	0.0584 ± 0.0143	7.18 ± 1.24	26.2 ± 1.6
270	0.0071 ± 0.0039	0.0258 ± 0.0122	0.828 ± 0.055	0.0194 ± 0.0039	0.144 ± 0.020	7.73 ± 0.94	10.6 ± 0.8
570	0.0224 ± 0.0060	0.074 ± 0.0149	0.631 ± 0.045	0.0254 ± 0.0072	0.239 ± 0.047	3.92 ± 0.72	7.3 ± 0.7
1500	0.0075 ± 0.0030	0.0739 ± 0.0114	0.249 ± 0.020	0.0122 ± 0.0025	0.449 ± 0.021	1.66 ± 0.23	2.4 ± 0.4
2500	0.0045 ± 0.0042	0.109 ± 0.013	0.102 ± 0.012	0.017 ± 0.0046	0.522 ± 0.042	0.54 ± 0.05	3.2 ± 0.5
3400	nd	0.137 ± 0.017	0.307 ± 0.026	0.0215 ± 0.0065	0.583 ± 0.066	4.56 ± 0.49	6.1 ± 0.6
4000	0.0154 ± 0.0048	0.142 ± 0.019	0.464 ± 0.034	0.0112 ± 0.0080	0.510 ± 0.055	3.97 ± 0.39	7.2 ± 0.5
Sta. 370 (85°54.9'N, 22°44.1'E, 4810 m)							
6	0.0377 ± 0.0053	0.0204 ± 0.0084	1.61 ± 0.07	0.0298 ± 0.0047	0.097 ± 0.015	—	⋮
150	0.0065 ± 0.0018	0.0096 ± 0.0096	1.22 ± 0.02	0.0189 ± 0.0038	0.136 ± 0.034	—	—
275	0.0084 ± 0.0026	0.0227 ± 0.0102	1.08 ± 0.02	0.0294 ± 0.0080	0.210 ± 0.034	—	—
550	0.0076 ± 0.0019	0.0545 ± 0.0076	1.34 ± 0.02	0.0123 ± 0.0055	0.355 ± 0.052	—	—
1500	0.0018 ± 0.0019	0.0528 ± 0.0091	0.355 ± 0.012	0.0122 ± 0.0052	0.420 ± 0.055	—	—
2500	0.0069 ± 0.0034	0.0725 ± 0.0106	0.325 ± 0.022	0.0100 ± 0.0035	0.489 ± 0.034	—	—
3500	0.0094 ± 0.0057	0.233 ± 0.018	1.32 ± 0.06	0.0394 ± 0.0103	0.367 ± 0.046	—	—
4500	0.0177 ± 0.0039	0.240 ± 0.019	1.38 ± 0.06	0.0334 ± 0.0072	0.229 ± 0.034	—	—
Sta. 423 (81±19.9'N, 15±18.9'E, 2245 m)							
6	0.239 ± 0.015	0.175 ± 0.017	0.934 ± 0.037	0.0678 ± 0.0156	0.0895 ± 0.0347	—	—
250	0.0179 ± 0.0038	0.0207 ± 0.0094	1.06 ± 0.04	0.0364 ± 0.0117	0.116 ± 0.035	—	—
750	0.033 ± 0.0052	0.064 ± 0.0090	0.943 ± 0.048	0.0178 ± 0.0047	0.147 ± 0.027	—	—
1400	0.0281 ± 0.0041	0.0886 ± 0.0102	0.459 ± 0.025	0.0170 ± 0.0041	0.248 ± 0.029	—	—
1650	0.0251 ± 0.0055	0.138 ± 0.015	0.557 ± 0.032	0.0377 ± 0.0052	0.310 ± 0.025	—	—
1900	0.0474 ± 0.0066	0.232 ± 0.021	0.768 ± 0.040	0.0191 ± 0.0052	0.309 ± 0.034	—	—

nd: Not detected.

Table 2.   *Retention of thorium isotopes on prefilters in series*
(Sta. 423*)*

Depth (m)	^{232}Th	^{230}Th
PFB/PFA (dpm/dpm)		
6	$0.044 \pm .032$	$0.062 \pm .078$
1400	1.63 ± 0.41	$0.491 \pm .166$
1650	$0.387 \pm .140$	$0.091 \pm .067$
1900	$0.170 \pm .058$	$0.091 \pm .043$
PFB/(PFA + PFB) (dpm/dpm)		
6	$0.042 \pm .031$	$0.059 \pm .074$
1400	0.620 ± 1.160	$0.329 \pm .113$
1650	$0.279 \pm .095$	0.083 ± 061
1900	$0.146 \pm .049$	$0.084 \pm .040$
PFB/Dissolved (dpm/dpm)		
6	0.154 ± 118	0.122 ± 160
1400	$2.69 \pm .87$	$0.175 \pm .059$
1650	$0.257 \pm .082$	$0.040 \pm .029$
1900	$0.422 \pm .174$	$0.069 \pm .033$

PFB/PFA: ratio of activity on second 0.5 μm wound fiber
cartridge prefilter to first prefilter in series. PFB/(PFA $\pm$
PFB): ratio of activity on second prefilter to total activity
retained on both prefilters. PFB/Dissolved: ratio of activity
on second prefilter to dissolved activity calculated from
manganese dioxide-loaded cartridges.

the Nansen Basin via the Fram Strait. Thus

$$^{226}Ra = [(1.71 \pm 0.11)Si + 74.2 \pm 0.9]\frac{S}{35} \qquad (2)$$

Where ^{226}Ra is the ^{226}Ra activity (dpm/1000 kg); Si is dissolved Si (μmol/kg); S is salinity
(‰)

The constants $(1.71 \pm 0.11)\frac{dpm^{226}Ra}{\mu molSi}$ and $74.2 \pm 0.9\frac{dpm}{1000kg}$ were obtained from the best fit
relationship of ^{226}Ra vs Si at TTO Stas 142–162. Values of ^{228}Ra calculated using equation
(2) and measured ^{228}Ra/^{226}Ra ratios (reported in Rutgers van der Loeff *et al.*, 1995) are
given in Table 1.

Following the initial Th separation, the Ra fractions from a few of the manganese
cartridges were retained for determination of ^{228}Ra by the ^{228}Th ingrowth method (Moore
et al., 1985). The mean Ra extraction efficiency ($\pm 1\sigma$) determined for these samples was 31.3
$\pm$ 7.2%. This value, together with the calculated ^{228}Ra activities (Table 1), has been used to
correct the ^{228}Th activities to sample collection. Stations 287 and 358 were analyzed
promptly after sample collection and the corrections are minimal (generally $\leq 15\%$) for
these samples. The dissolved ^{228}Th analyses at Stas 370 and 423 entail significant Ra
ingrowth corrections and are not presented.

Table 2 gives ^{232}Th and ^{230}Th data on the paired prefilters deployed in series on four
pumps at Sta. 423. Relative to the total activity retained on the two filters (PFB/PFB +
PFA), the fraction on the second prefilter generally was $\leq 33\%$. Greater proportions were

noted on the samples collected at 1400 m. The proportion of ^{232}Th retained on the second prefilter is consistently greater than that of ^{230}Th relative to either the total particulate (PFA + PFB) or "dissolved" activities. ^{232}Th has no in-situ source in the oceans and is added in association with particles; the observation of greater proportions of ^{232}Th than ^{230}Th on the second prefilter makes it likely that the Th activity on the second prefilter is due to particles which pass the first and are retained on the second prefilter. For ^{230}Th, however, this fraction (PFB/Dissolved; Table 2) is $\leq 18\%$ of the dissolved ^{230}Th activity calculated from the two manganese oxide cartridges. For ^{232}Th, the fraction is generally $\leq 40\%$, but is greater in the 1400 m sample. Thus "leakage" of particles through the prefilter does not contribute significantly to the dissolved ^{230}Th in a typical deployment consisting of one prefilter and two Mn-treated cartridges, but the "dissolved" ^{232}Th values must be viewed as upper limits.

Total ^{210}Pb activities measured on aliquots from large volume water samples (Table 3) show relatively little variation with depth. The anthropogenic radionuclide data are given in Tables 4 and 5. For ^{137,134}Cs and ^{239,240}Pu, total activities are determined from the 60 l samples. Americium-241 activities are determined from the in-situ pump samples and utilize

Table 3. ^{210}Pb data for Nansen Basin water samples

Depth (m)	Total ^{210}Pb* (dpm/1000kg) kg)	^{226}Ra† (dpm/1000kg)
Sta. 340 (82 59'N, 31 58.6'E, 3800 m)		
100	32.8 ± 3.2	80.7
450	44.5 ± 4.2	84.4
750	30.9 ± 3.6	86.6
1100	30.8 ± 4.5	89.7
1500	36.9 ± 4.7	91.4
1800	52.4 ± 6.3	92.7
2200	36.5 ± 5.4	93.6
2800	25.9 ± 3.3	93.8
3400	47.9 ± 4.9	94.4
3750	32.2 ± 3.9	94.6
3800	29.2 ± 4.5	94.6
Sta. 371(86 7.9'N, 22 4.3'E, 3945 m)		
6	87.1 ± 1.8	75.4
100	45.6 ± 5.4	78.2
250	34.1 ± 4.8	83.5
450	27.5 ± 4.6	84.4
850	33.8 ± 4.7	85.7
1300	29.4 ± 3.9	88.3
1900	31.5 ± 4.4	91.7
2500	215 ± 2.2	92.7
3100	39.7 ± 3.0	93.4
3800	39.1 ± 3.1	93.6
3900	27.0 ± 3.0	93.6
3930	27.4 ± 2.9	93.6

*Dissolved plus particulate.
†Calculated from correlation between dissolved silicate and ^{226}Ra (see text).

Table 4.   Americium and plutonium analyses of Nansen Basin water
samples

Depth (m)	241Am (dissolved) (dpm/1000 l)	239.240Pu (total) (dpm/1000 l)
Sta. 287		
6	0.116 ± 0.014*	1.07 ± 0.12*
350	0.113 ± 0.013*	1.75 ± 0.16*
500	0.097 ± 0.015	1.61 ± 0.13
800	——	1.60 ± 0.13
1050	0.138 ± 0.011	—
1300	——	1.62 ± 0.14
1450	0.129 ± 0.018	—
1900	——	1.20 ± 0.10
2050	0.043 ± 0.020	—
2150	0.036 ± 0.027	—
Sta. 358		
20	——	1.00 ± 0.14
270	0.137 ± 0.009	1.14 ± 0.16
570	0.248 ± 0.044	1.44 ± 0.17
1120	——	1.16 ± 0.14
1500	0.148 ± 0.010	—
2500	0.062 ± 0.009	0.54 ± 0.06
3400	0.027 ± 0.008	0.11 ± 0.08
3950	——	0.57 ± 0.06
4000	0.018 ± 0.006	0.76 ± 0.09

* Particulate 241Am: 6 m, 0.006 ± 0.001 dpm/1000 l; 350 m, 0.011
± 0.002 dpm/1000 l.

the cartridge extraction efficiency calculated from the Th data. Previous work has shown that Am and Th behave similarly with respect to their uptake on the Mn-impregnated cartridges (Cochran et al., 1987).

DISCUSSION

Scavenging of reactive radionuclides—thorium isotopes and ^{210}Pb

In the Arctic Ocean, low particle concentrations and fluxes often have been cited as causing low scavenging efficiency of reactive radionuclides. Ku and Broecker (1967) advanced this hypothesis to explain the anomalously low ^{230}Th and ^{231}Pa inventories in a deep-sea sediment core collected under ice island T-3 and Finkel et al. (1977) similarly used the argument to explain low ^{10}Be inventories in Arctic Ocean cores. More recently Moore and Smith (1986) and Bacon et al. (1989) used water column data to show that scavenging of ^{230}Th, ^{210}Po and ^{210}Pb is slower in the Canada Basin than in the Atlantic Ocean.

In contrast, the central Nansen Basin ^{230}Th profiles (Stas 358, 370; Fig. 2) are similar to those observed in the open North Atlantic Ocean (Cochran et al., 1987). At Station 358, dissolved ^{230}Th increases to relatively constant values of ~0.5–0.6 dpm/1000 l at depths greater than 2500 m (Fig. 2). The ratio of particulate to dissolved ^{230}Th ranges from 0.13 to 0.25, also similar to the north-west Atlantic. The profile at Sta. 358 is comparable to one
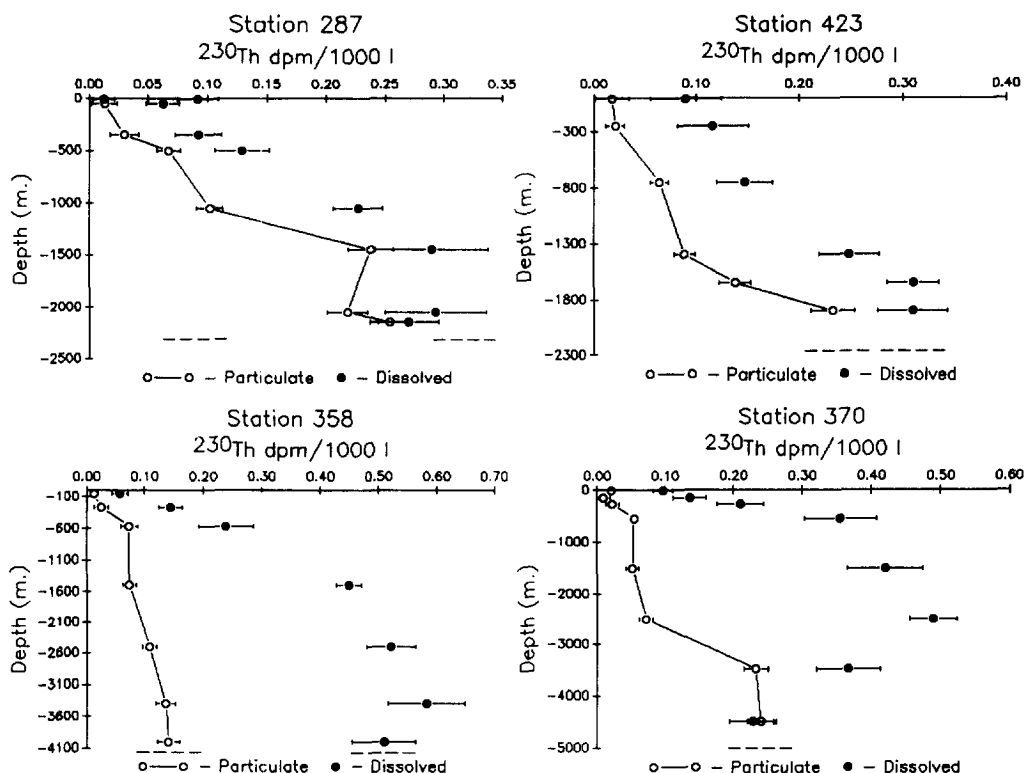
Fig. 2.   Thorium-230 profiles obtained from in-situ pump casts at four stations in the Nansen Basin:
Sta. 287, 423—Barents Sea slope, Sta. 358—Central Basin, Sta. 370—Gakkel Ridge. Dashed lines
indicate bottom depths; open circles indicate particulates (> 0.5 μm); filled circles indicate dissolved
material.

obtained from the central Nansen Basin in 1991 (Scholten *et al.*, 1994), indicating good
intercalibration. At Sta. 370 in the vicinity of the Gakkel Ridge, dissolved ^{230}Th increases to
~0.5 dpm/1000 l at a depth of about 2500 m then decreases toward the bottom. This
decrease in dissolved ^{230}Th is complemented by a marked increase in particulate ^{230}Th,
suggesting enhanced scavenging associated with the ridge (Kadko *et al.*, 1986; Shimmield
and Price, 1988). Indeed Schlosser *et al.* (1990) have identified the Gakkel Ridge as a
possible source of primordial ^{3}He to the deep Nansen Basin, and hydrothermal activity or
nepheloid layers associated with the ridge may explain the enhanced removal of ^{230}Th.

In the marginal areas of the Nansen Basin, scavenging of ^{230}Th is enhanced relative to the
basin interior. This is seen at Sta. 287, taken close to the Barents Sea continental slope (Fig.
2), where dissolved ^{230}Th activities do not exceed 0.3 dpm/1000 l. Particulate activities also
show high values, producing particulate/dissolved ^{230}Th ratios ranging from 0.1 to 0.6, a
factor of about 2 greater than in the central basin. Similarly, dissolved ^{230}Th is low and the
proportion of particulate to dissolved ^{230}Th is high at Sta. 423, taken near the slope off
Svalbard.

These trends in ^{230}Th are reflected in the ^{228}Th data (Fig. 3). The two stations for which
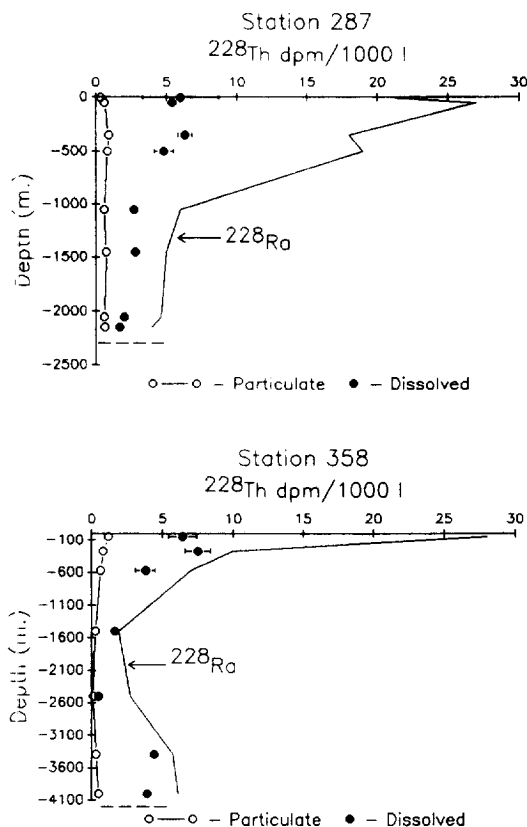dissolved ^{228}Th could be calculated reliably, 287 and 358, provide examples of both basin

Fig. 3. Thorium-228 profiles at the Barents Sea slope (Sta. 287) and Central Nansen Basin (Sta. 358). Open circles indicate particulates (> 0.5 μm); filled circles indicate dissolved ^{228}Ra activities (solid line) determined from measured ^{228}Ra/^{226}Ra activity ratios (Rutgers van der Loeff *et al.*, 1995) and calculated ^{226}Ra activities (see text). Dashed lines indicate bottom depths.

margin (Sta. 287) and central basin (Sta. 358) profiles. Particulate ^{228}Th is greater and dissolved ^{228}Th is somewhat lower at Sta. 287 than at 358. The total ^{228}Th is lower in the deep water column at Sta. 287 than at 358, indicating enhanced removal at Sta. 287. Both stations show low ^{228}Th/^{228}Ra activity ratios in the upper 50 m. At Sta. 358 the ratios approach equilibrium at depth, while at Sta. 287 they remain < 0.6.

Assuming that the Th isotope profiles are steady state, residence times for both dissolved and particulate Th can be calculated from the data (Coale and Bruland, 1987). The residence time of dissolved Th with respect to scavenging onto particles, τ_d, is

$$\tau_d = \frac{1}{\lambda} \frac{A_d}{(P - A_d)} \tag{3}$$

where λ is the Th decay constant (year^{-1}), A_d is the dissolved ^{228}Th or ^{230}Th activity (dpm/l) and P is the parent activity (^{228}Ra or ^{234}U; dpm/l)

The residence time of particulate Th is

$$\tau_p = \frac{A_p}{\lambda[P - (A_d + A_p)]} \qquad (4)$$

where A_p is the particulate [228]Th or [230]Th activity (dpm/l).

Equations (3) and (4) both depend on the extent of disequilibrium between parent and daughter Th isotope. In the Nansen Basin deep water, [228]Th is close to equilibrium with [228]Ra ([228]Th/[228]Ra ~ 0.8) and is consequently not a useful tracer for calculating τs. In the surface water, [228]Th/[228]Ra disequilibrium is greater and this isotope can be used. Thorium-230 displays disequilibrium relative to [234]U throughout the water column, but in the surface water "dissolved" [230]Th activities are low and often are not significantly greater than "dissolved" [232]Th (Figs 3 and 4). Both [230]Th and [232]Th can be present in the "dissolved" fraction in surface waters by leaching of atmospherically supplied dust particles (Cochran *et al.*, 1987) or through particles finer than 0.5 μm that pass the prefilter but may be retained on the manganese cartridges. The correction for [234]U-supported [230]Th is large in these samples and [230]Th is consequently not a sensitive tracer for calculating scavenging rates in surface water.
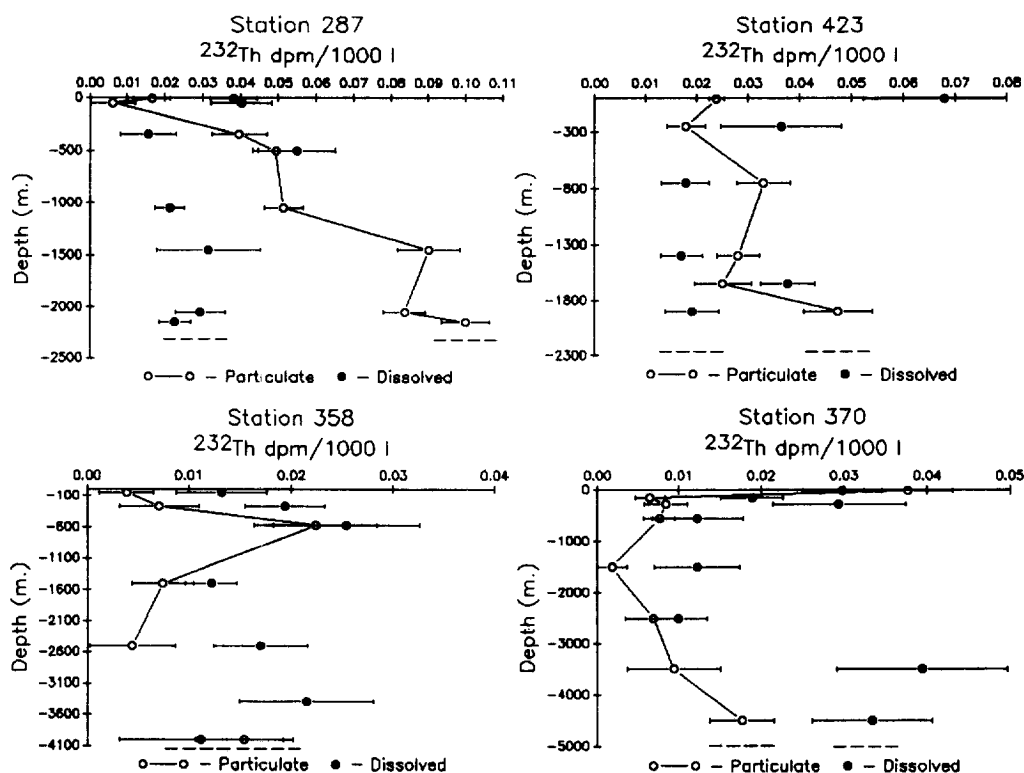

Fig. 4. Particulate and dissolved [232]Th profiles in the Nansen Basin. Open circles indicate particulates (> 0.5 μm); filled circles indicate dissolved material; dashed lines indicate bottom depths.

Table 5 gives residence times for dissolved and particulate Th in surface water (calculated from ^{228}Th/^{228}Ra disequilibrium) and deep water (calculated from ^{230}Th/^{234}U disequilibrium) for the stations sampled. Corrections for supported ^{230}Th were made to the particulate activities by assuming that the activity ratio of supported ^{230}Th to ^{232}Th is 0.6 (R. Anderson, personal communication). This correction is generally $\leq$10% of the particulate ^{230}Th activity in the central basin and ranges up to 25% at Sta. 287. The Eurasian Basin Deep Water (Stas 358 and 370) has a dissolved Th residence time with respect to scavenging of 18–19 years. Within the Gakkel Ridge complex, the value drops to $\sim$ 12 years near the bottom. Dissolved ^{230}Th in deep water of the Barents Sea slope has mean residence times of $\sim$10.5–12 years, indicating more rapid removal onto particles in this ocean margin environment. Particulate Th residence times are longer ($\sim$ 6 years) in the slope deep water relative to the basin interior ($\sim$ 2–4 years), probably indicating greater particle resuspension rates caused by slope boundary currents. In the surface water, dissolved Th has a mean residence time of about 1 year in both central basin and slope environments, and particulate Th is removed rapidly (0.06–0.2 years).

The mean residence time of total ^{210}Pb with respect to scavenging and particle removal also may be calculated using a variation of equation (4):

$$\tau_{Pb} = 32.3 \frac{A_{Pb}}{(A_{Ra} - A_{Pb})} \tag{5}$$

Data are available for two central basin stations, 340 and 371 (Fig. 5). Total ^{210}Pb activities in the deep water (1500–3000 m) average 35 $\pm$ 10 dpm/1000 l. Relative to average ^{226}Ra activities of $\sim$ 93 dpm/1000 l (Table 3), τ_{Pb} is about 19 years. This value is similar to that for the North Atlantic (Cochran *et al.*, 1990).

The general increases in both dissolved and particulate ^{230}Th with depth support the hypothesis that a sorption equilibrium is occurring between dissolved and particulate Th (Nozaki *et al.*, 1981; Bacon and Anderson, 1982; Bacon *et al.*, 1985; Nozaki *et al.*, 1987; Bacon *et al.*, 1989). Using box models of the dissolved and particulate forms of ^{230}Th and ^{228}Th gives

$$\frac{A_p}{A_{d228}} = \frac{k_1}{k_{-1} + \lambda_{228}} \tag{6}$$

$$\frac{A_p}{A_{d230}} \geq \frac{k_1}{k_{-1}} \tag{7}$$

where A_p is the particulate ^{230}Th or ^{228}Th (dpm/1000 l), A_d is the dissolved ^{230}Th or ^{228}Th (dpm/1000 l), k_1 is the adsorption rate constant (year^{-1}), k_{-1} is the desorption rate constant (year^{-1}), λ_{228} is the decay constant for ^{228}Th (0.3647 year^{-1}).

Equation (7) assumes that $\lambda_{230} \ominus k_{-1}$, and if λ_{228} is comparable to k_{-1}, individual values for k_1 and k_{-1} can be calculated from the data. If $\lambda_{228} \ominus k_{-1}$, only the quotient k_1/k_{-1} can be calculated.

The mean A_p/A_d values below 500 m (Table 1), corrected for supported particulate Th using ^{232}Th, are: $A_p/A_d \Theta^{228} = 0.23 \pm 0.06$ and 0.13 ± 0.04, and $A_p/A_d\Theta_{230} = 0.51 \pm 0.19$ and 0.22 ± 0.04 for Stas 287 and 358, respectively. From equations (6) and (7), we obtain $k_1 = 0.15 \pm 0.07$ and 0.12 ± 0.07 year^{-1} and $k_{-1} = 0.29 \pm 0.17$ and 0.55 ± 0.34 year^{-1} at Stas 287 and 358, respectively. The large errors associated with the estimates of k_1 and k_{-1}

Table 5. Residence times for dissolved and particulate Th

Location	^{228}Th				^{230}Th			
	A_{part} (10^{-3}dpm/l)	τ_{part} (year)	A_{diss} (10^{-3}dpm/l)	τ_{diss} (year)	A_{part}* (10^{-3}dpm/l)	τ_{part} (year)	A_{diss} (10^{-3}dpm/l)	τ_{diss} (year)
Nansen Basin								
Sta. 358 (Central Basin)								
Surface water (<50 m)	1.2 ± 0.06	0.20 ± 0.01	7.2 ± 1.2	1.0 ± 0.13	—	—	—	—
EBDW (1500–2500 m)†	—	—	—	—	0.088	3.4	0.486	18.9
EBBW (3400–4000m)†	—	—	—	—	0.135	5.3	0.546	21.2
Sta. 370 (Gakkel Ridge)								
EBDW (1500–2500 m)†	—	—	—	—	0.060	2.3	0.455	17.7
EBBW (3500–4500 m)†	—	—	—	—	0.228	8.9	0.298	11.6
Barents Sea Slope								
Sta. 287								
Surface water	0.341 ± .041	0.06 ± 0.01	7.3 ± 3.3	1.1 ± 0.5	—	—	—	—
Deepwater (1450–2150 m)	—	—	—	—	0.182 ± 013	7.1 ± 0.5	0.270 ± .030	10.5 ± 1.2
Sta. 423								
Deepwater (1650–1900 m)	—	—	—	—	0.163	5.8	0.310	12.1

Activities are average activities for the depths indicated.

*Corrected for supported ^{230}Th using measured particulate ^{232}Th activities and assuming (U-supported ^{230}Th/^{232}Th) activity ratio in particles = 0.6.

†EBDW = Eurasian Basin Deep Water; EBBW = Eurasian Basin Bottom Water.

Station 340
Activity dpm/1000 kg

O — 210Pb   ● — 226Ra

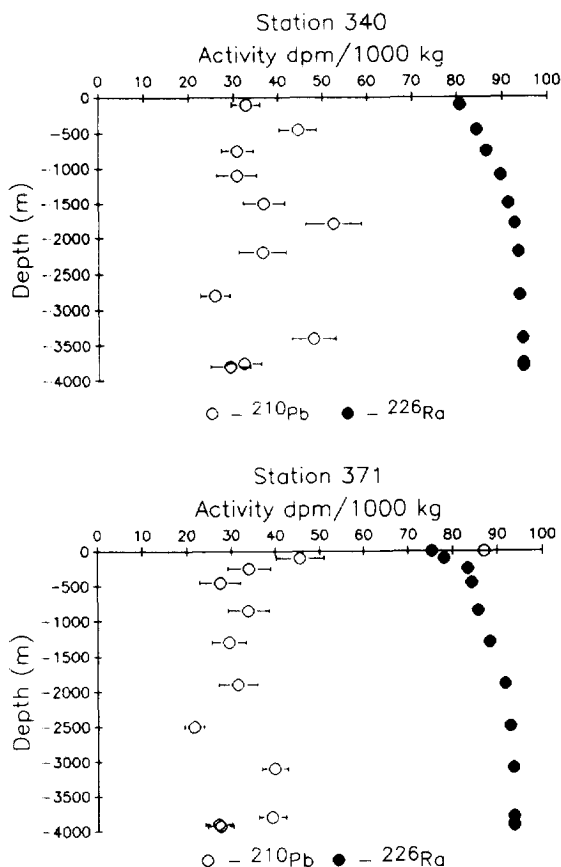Station 371
Activity dpm/1000 kg

O — 210Pb   ● — 226Ra

Fig. 5. Total [210]Pb (particulate + dissolved; open circles) at two stations in the Nansen Basin. Sta. 340—Central Basin, Sta. 371—Gakkel Ridge. Filled circles [226]Ra activity calculated from Ra vs Si correlation (see text).

make it difficult to discern differences at the two stations. However, the calculated values of k_1 and k_{-1} are within the range of values from open ocean sites in the North Atlantic and North Pacific (Murnane et al., 1994) and reinforce the notion that scavenging of Th is not markedly different in the Nansen Basin from the Atlantic or Pacific.

Although the residence times calculated for Th in the Nansen Basin surface water are not significantly different from values obtained for the open North Atlantic Ocean (Kaufman et al., 1973; Broecker et al., 1973; Li et al., 1980), they do stand in contrast with the results of Bacon et al. (1989), who found Th residence times of 6 years in the surface waters of the Alpha Ridge, separating the Canada and Makarov Basins. In the deep water, Th residence times of about 20 years in the central Nansen Basin are significantly shorter than values of 55 years estimated by Scholten et al. (1994) for the Makarov Basin. Several factors may explain these differences: (i) particle fluxes are greater in the Nansen Basin than in the Makarov Basin; (ii) ventilation time scales are more rapid for the Nansen Basin than the Makarov Basin; (iii) the Nansen Basin margin, specifically the Barents Sea slope, is a site of enhanced removal of Th and this sink influences the basin's interior.

There are few data on particle fluxes in the Arctic Ocean, but given the ice coverage of both the Amerasian (Canada and Makarov) and Eurasian (Amundsen and Nansen) Basins there seems no reason to expect particle fluxes to be different *a priori*. There are, however, well documented differences in ventilation times of the basins. In the Nansen Basin, the chlorofluoromethane (freon) data of Wallace *et al.* (1992) show detectable F-11 data throughout the water column at stations along the Barents slope (Sta. 287) and Gakkel Ridge (Sta. 370), with deep water (1000–3000 m) ages of 15–30 years. At Sta. 358 in the basin interior, deep water ages are about 5 years older than at the basin boundaries. FREON is undetectable in the Eurasian Basin bottom water (EBBW: > 3000 m), but this water mass has measurable CCl_4 and tritium, with a $T/^3He$ age of 40–50 years (Schlosser *et al.*, 1990). However, the radiocarbon age of this water is 200–250 years (Schlosser *et al.*, 1990). Even in the central Nansen Basin, water column FREON inventories are relatively high compared with the central Canada Basin, indicating more rapid ventilation of the former (Wallace and Moore, 1985; Wallace *et al.*, 1992). Indeed, ventilation of Nansen Basin Deep Water on a timescale not very different from the scavenging residence time of Th will tend to cause the ^{230}Th profiles to reach a constant value, as observed (Fig. 2), rather than the linear increase seen in the deep Pacific for example (Nozaki *et al.*, 1981). The ^{230}Th activity of the basin deep water thus represents a balance between in-situ production, scavenging and mixing with water with low ^{230}Th.

Our data also show evidence that removal of ^{230}Th is enhanced at the Barents Sea slope stations (287 and 423). Total ^{230}Th is slightly lower at these stations than in the basin interior (Sta. 358), but greater differences are apparent between dissolved and particulate activities. Enhanced scavenging of Th near the margin of the Nansen Basin may be due in part to higher particle concentrations and fluxes there. Although particle concentration data are not available for the ARK IV/3 samples, evidence for high values near the margin is seen in the particulate ^{232}Th distributions (Fig. 4). Unlike ^{230}Th and ^{228}Th, ^{232}Th is not produced *in situ* in the oceans, but rather is added in association with continentally-derived detrital particles. The concentrations of particulate ^{232}Th at the margin Stas 287 and 423 are factors of 3 to 8 greater than those at the interior Stas 358 and 370 (Table 1). Elevated particle concentrations near the basin margin, if coupled with greater particle fluxes, could produce enhanced removal of reactive radionuclides from the water column.

Americium-241 and $^{239,240}Pu$ distributions

The distributions of the transient tracers ^{241}Am and $^{239,240}Pu$ provide additional information on the pattern of scavenging suggested from Th isotope distributions in the Nansen Basin. At the Barents Sea slope station (287), Pu shows a broad maximum over the depth interval 350–1300 m. Americium-241 activities display more variation within this depth range, with a maximum at ∼ 1000 m (Fig. 6). In contrast, both Pu and Am show distinct maxima at ∼ 600 m in the central Nansen Basin (Sta. 358; Fig. 6). Moreover, $^{241}Am/^{239,240}Pu$ ratios are lower at the Barents slope than in the central Nansen Basin.

These patterns must be viewed in the context of the sources of these anthropogenic radionuclides to the Arctic. Livingston *et al.* (1984) have identified two important sources as direct atmospheric fallout from the testing of atomic weapons and advective supply from the North Atlantic. The former arrived in the period 1956–1966 with a peak in 1963–1964, and the latter is a continuous input that has varied over time due to the contribution of the discharge of these radionuclides from the nuclear fuel reprocessing facilities at Sellafield,
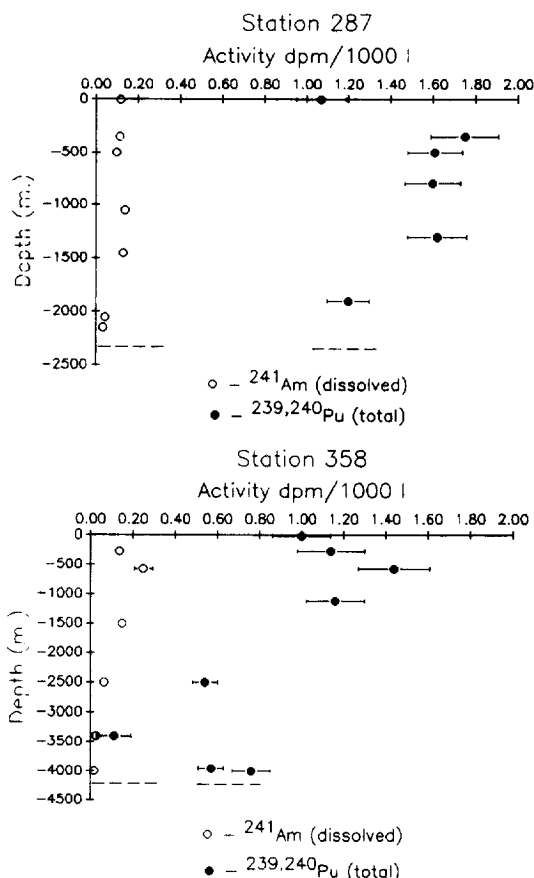
Fig. 6.   Americium-241 (dissolved) and ^{239,240}Pu (total) profiles in the Nansen Basin. Sta. 287—
Barents Sea slope, Sta. 358—Central basin Samples for ^{241}Am were collected using *in situ* pumps and
samples for Pu were taken from large volume water casts at the same stations.

U.K. (Livingston *et al.*, 1982). Sellafield inputs of ^{137}Cs, ^{239,240}Pu and ^{241}Am were
particularly high from 1974 to 1978, and during the period 1969–1978 greatly exceeded
the fallout delivery (Livingston *et al.*, 1984). An additional source of ^{137}Cs was the
Chernobyl reactor accident in April 1986 (see discussion below). The ^{239,240}Pu inventories at
Stas 287 and 358 are ~50 Bq/m^2 (Table 6), about a factor of 10 greater than the direct
fallout input at these latitudes (Livingston *et al.*, 1984).

Livingston *et al.* (1984) documented the presence of Sellafield ^{137}Cs in the Amundsen
Basin and determined a transit time of about 5 years from the Irish Sea to the Barents Sea
and an additional 3 years to the Amundsen Basin, the northernmost basin of the Eurasian
Basin (Fig. 1). Tritium/helium (Schlosser *et al.*, 1990) and chlorofluoromethane data
(Anderson *et al.*, 1989; Wallace *et al.*, 1992) also indicate fairly rapid ventilation (< 50 years)
of the Nansen Basin for depths less than 3500 m (see below). Thus it is likely that the
^{239,240}Pu distributions in the Nansen Basin are continuing to evolve, but have been
characterized by high inventories since the 1970s.

Table 6. *Anthropogenic radionuclide inventories in the Arctic and north-west Atlantic oceans*

	Reference	Water Depth (m)	Date	$\Sigma^{239,240}Pu$ (Bq/m^2)	$\Sigma^{241}Am$ (Bq/m^2)	Am/Pu (Bq/m^2)	$\Sigma^{137}Cs$ pre-Chernobyl	$\Sigma^{137}Cs$ post-Chernobyl
Arctic Ocean								
Nansen Basin (Sta. 358)	This study	4050	1987	52	7.3	0.14	7811	8749
Barents Sea Slope (Sta. 287)	This study	2250	1987	55	3.9	0.07	8367	13,740
Fram Basin	Livingston *et al.* (1984)	4000	1979	35	6.4	0.18	6790	—
Makarov Basin	Livingston *et al.* (1984)	4000	1979	24	6.2	0.26	3670	—
Northwest Atlantic Ocean								
Nares Abyssal Plain	Cochran *et al.* (1987)	5840	1984	44	12	0.27	2920	—
Hatteras Abyssal Plain	Cochran *et al.* (1987)	5400	1980–81	93	13	0.14	4770	—

Americium-241 shows the opposite trend from Pu or ^{137}Cs, namely higher activities and water column inventories in the central basin (Sta. 358) than at the margin (Sta. 287, Table 6). Because ^{241}Am is produced from ^{241}Pu decay, this pattern can be explained in the context of rapid supply of Pu to the Nansen Basin via the Barents Sea followed by production of ^{241}Am in the lower scavenging environment of the central basin. Americium-241 that accompanied the Pu or was produced *en route* was likely scavenged in the rapid scavenging regimes of the Barents shelf or slope, consistent with the observation of lower ^{241}Am inventories at slope Sta. 287.

Mixing timescales in the Nansen Basin: Evidence from Cs isotope distributions

We have argued that the particle-reactive tracer distributions in the Nansen Basin are affected by the relatively rapid mixing or ventilation timescales for the Eurasian Basin Deep Water (EBDW). These timescales are estimated to be less than about 50 years, based on FREON, CCl$_4$ and T/^{3}He distributions (Wallace *et al.*, 1992). The cesium isotope data provide additional constraints on ventilation timescales of the Nansen Basin.

Two important sources of ^{137}Cs to the Arctic Ocean are direct fallout from nuclear weapons testing and Cs advected from the Sellafield reprocessing facility (Livingston *et al.*, 1984, 1985). The ARK IV/3 cruise was about one year after the accident at the Chernobyl nuclear power generating station, and the Chernobyl accident constitutes another potential source of ^{137}Cs to the Nansen Basin. The presence of Chernobyl-derived Cs is evident in the high $^{134}Cs/^{137}Cs$ activity ratios in the upper water column (0.1–0.2, Table 7). In comparison, corresponding pre-Chernobyl $^{134}Cs/^{137}Cs$ ratios measured in the same area in 1981 did not exceed 0.03 (Casso and Livingston, 1984). The Sellafield source term has been declining, and the $^{134}Cs/^{137}Cs$ would have decreased to ≤ 0.005 in 1987 in the absence of Chernobyl input. The short half-life of ^{134}Cs (2.1 years) places constraints on the rate of mixing, and we note that ^{134}Cs is present to 1000 m at the Barents slope stations (287, 423, Fig. 7) but is mixed to

J. K. Cochran *et al.*

Table 7. Cesium isotope data for Nansen Basin water samples

| Depth	^{137}Cs (dpm/1000 l)	^{134}Cs	Pre-Chernobyl ^{137}Cs (dpm/1000 l)
Sta. 287			
6	702 ± 24	82 ± 7	477 ± 27
50	708 ± 9	78 ± 2	495 ± 11
100	631 ± 22	65 ± 6	453 ± 25
350	702 ± 16	78 ± 4	489 ± 21
400	583 ± 14	62 ± 3	412 ± 16
500	599 ± 10	70 ± 3	407 ± 12
800	149 ± 7	2.2 ± 1.1	143 ± 8
1050	150 ± 7	0.8 ± 1.3	148 ± 8
1450	95 ± 7	−0.1 ± 1.6	95 ± 8
1850	64 ± 1	−0.6 ± 2.0	64 ± 1
2050	61 ± 4	−0.9 ± 1.9	61 ± 4
2150	61 ± 8	−1.1 ± 3.0	61 ± 8
Sta. 358			
6	762 ± 8	9.4 ± 1.2	737 ± 8
50	1090 ± 10	105 ± 4	803 ± 13
270	440 ± 5	5.9 ± 0.6	423 ± 5
400	384 ± 10	−0.1 ± 1.3	384 ± 10
570	240 ± 8	1.3 ± 1.3	236 ± 8
870	193 ± 37	−15 ± 16	193 ± 37
1500	59 ± 4	0.1 ± 1	59 ± 4
2482	17 ± 2	—	16 ± 4
2500	11 ± 1	0 ± 0.8	10 ± 2
3100	6 ± 2	1.8 ± 1.7	0.5 ± 1.0
3372	11 ± 2	—	9 ± 2
3400	8 ± 4	0.6 ± 0.8	6 ± 2
3916	9 ± 2	—	6 ± 2
3950	15 ± 4	2.0 ± 2.1	101 ± 3
3966	14 ± 4	—	9 ± 4
4000	150 ± 10	48 ± 4	181 17
Sta. 370			
6	557 ± 7	4.4 ± 1	545 ± 7
275	401 ± 13	−0.6 ± 2.2	401 ± 13
550	204 ± 11	−1.2 ± 1.9	204 ± 11
1500	111 ± 5	1.5 ± 1.3	107 ± 5
2500	45 ± 3	−1.6 ± 10	45 ± 3
3500	31 ± 9	0.6 ± 3.4	29 ± 9
4500	27 ± 3	−1.2 ± 1	27 ± 3
Sta. 423			
6	859 ± 136	55.9 ± 9	706 ± 138
250	596 ± 95	46.3 ± 8	469 ± 197
750	353 ± 56	9.1 ± 1.9	328 ± 56
1400	69 ± 11	0.2 ± 0.8	69 ± 11
1650	51 ± 8	−0.6 ± 0.7	51 ± 8
1900	66 ± 11	0.4 ± 1.2	65 ± 11
2150	4 ± 8	—	4 ± 8
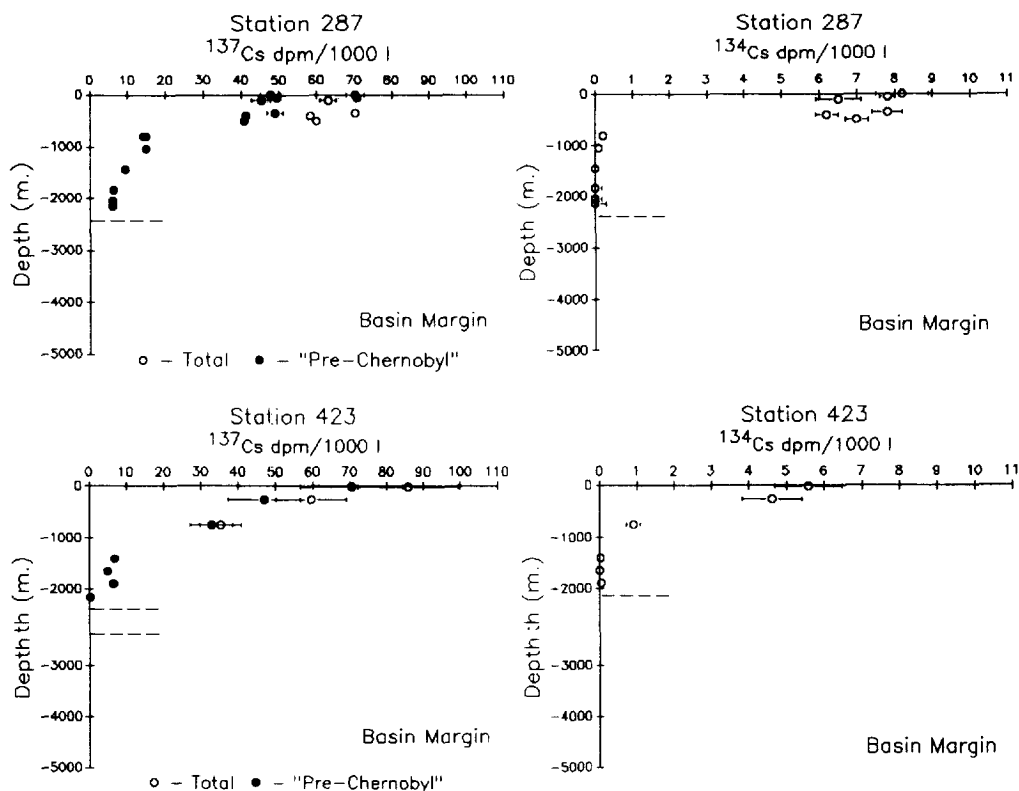
Fig. 7. Cesium-134 and ^{137}Cs profiles from the Nansen Basin. Open circles correspond to activities measured in samples collected in 1987. Filled circles indicate pre-Chernobyl ^{137}Cs activities calculated from [134]Cs data (see text).

depths of < 300 in the basin interior (Stas 358, 370, Fig. 7). Because about 1 year had elapsed since the introduction of this [134]Cs to the Nansen Basin, mixing of [134]Cs to these depths was accomplished within 1 year.

The EBDW at Stas 358 and 370 is generally unlabelled by Chernobyl Cs at the time of sampling, but an interesting exception to this pattern is the near-bottom sample at Sta. 358, which shows the highest [134]Cs/^{137}Cs measured at any of the stations (Fig. 7). Cesium is only weakly reactive in seawater (Bowen et al., 1980), but we attribute this high [134]Cs to Cs associated with particulate material from the Chernobyl accident that sank rapidly to the bottom. Although sea ice coverage of the Nansen Basin is heavy in the winter, breakup is common in the spring and summer, allowing particles trapped by the ice to enter the water column and sink. Moreover, Sta. 358 is located in one of the branches of the Transpolar Ice Drift, with most of the ice in this area originating in Siberian shelves in the Laptev Sea (Thiede, 1988; Anderson and Jones, 1992). It is possible that particulate Cs from Chernobyl could have labeled the ice in this area and been rapidly transported to Sta. 358.

The [134]Cs/^{137}Cs ratios, corrected for decay to the date of the Chernobyl accident, can be coupled with the [134]Cs/^{137}Cs ratio of Cs released by the accident to determine the "pre-Chernobyl" profile of ^{137}Cs at the four stations (Fig. 7; Table 7). The profiles show that pre-Chernobyl ^{137}Cs is present throughout the water column at the slope Stas 287 and 423, but is
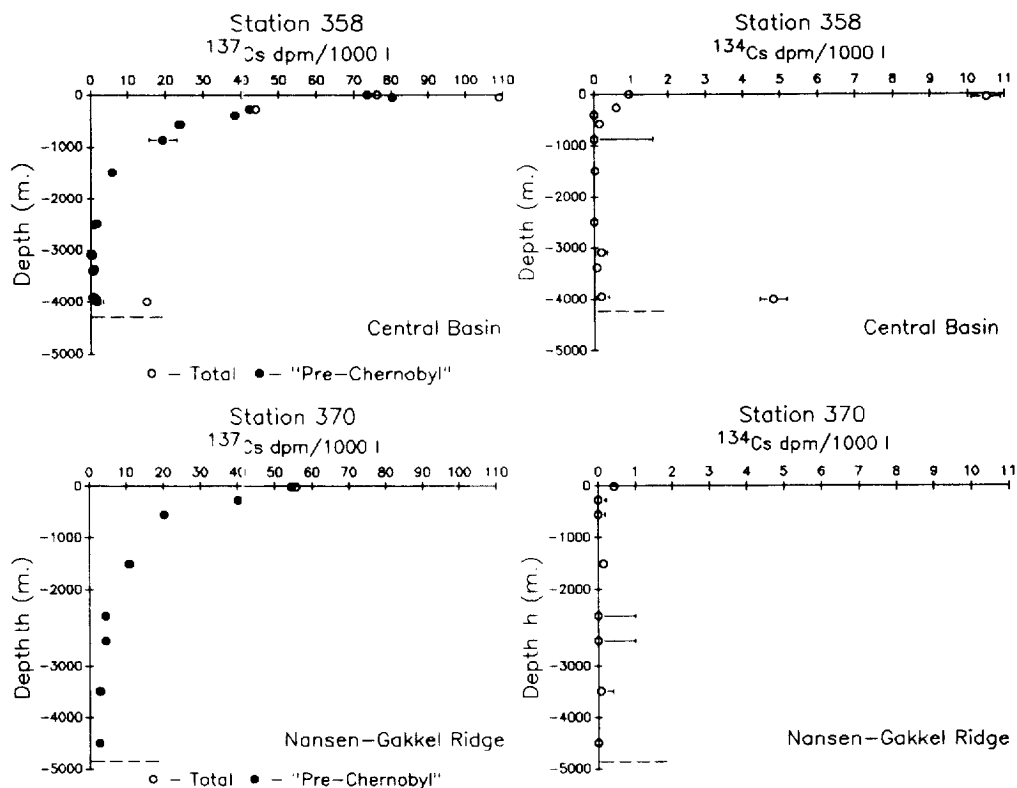
Fig. 7. *Continued.*

present at very low activities (≤ 10 dpm/1000 l) in the deep central basin. Station 370, the Gakkel Ridge station, shows higher ^{137}Cs at depth relative to Sta. 358, and this pattern is consistent with ^{228}Ra (Rutgers van der Loeff *et al.*, 1995) and freon data (Wallace *et al.*, 1992), which show deeper mixing in the vicinity of the Nansen Ridge. The presence of very low ^{137}Cs activities in the EBDW are consistent with the ages of about 50 years for this water estimated from T/^{3}He and CCl$_4$ distributions (Schlosser *et al.*, 1990; Wallace *et al.*, 1992).

Inventories of pre-Chernobyl ^{137}Cs in the Nansen Basin are greater than those measured in 1979 in the Fram and Makharov Basins (Table 6). The latter in turn are greater than those measured in the Northwest Atlantic in the early 1980s (Table 6). This pattern emphasizes the importance of the Sellafield source of ^{137}Cs to the Nansen Basin. The Barents Sea slope and Nansen Basin have been strongly labeled with this source to depths of at least 1500 m in the central basin and throughout the water column at the Barents slope. This implies ventilation timescales of 9–18 years for these waters, given the release pattern of ^{137}Cs from Sellafield (Livingston *et al.*, 1982).

CONCLUSIONS

The distributions in the Nansen Basin of the naturally occurring thorium isotopes ^{230}Th and ^{228}Th and the anthropogenic radionuclide ^{241}Am suggest that scavenging is less intense in the Eurasian Basin Deep Water in the central basin than at the basin margins (e.g. Barents

Sea slope). Residence times of dissolved Th in the basin deep water are 18–19 years in the central Nansen basin and 10–12 years on the Barents Sea slope. Mixing timescales are estimated from ^{134}Cs and ^{137}Cs distributions. Cesium-134 derived from the accident at the Chernobyl nuclear power station 1 year prior to sampling has been mixed to depths of 1000 m at the Barents Slope and to ~ 300 m in the central Nansen Basin. Pre-Chernobyl ^{137}Cs, derived from fallout from atmospheric testing of atomic weapons and the nuclear fueled reprocessing facility at Sellafield, U.K., has been mixed throughout the water column at all stations, but is present in very low activities in the Eurasian Basin Deep Water in the central Nansen Basin. This pattern is consistent with ages of about 50 years for this water mass, based on T/^{3}He and FREON distributions (Schlosser *et al.*, 1990; Wallace *et al.*, 1992). The relatively rapid mixing time of Eurasian Basin Deep Water in the Nansen Basin, coupled with the texture and rate of Th scavenging within the basin, maintains dissolved ^{230}Th activities at a lower value in the Nansen Basin compared with previously reported values in the deep Canadian Basin.

REFERENCES

Anderson L. G. and E. P. Jones (1992) Tracing upper waters in the Nansen Basin in the Arctic Ocean. *Deep-Sea Research*, **39**, S425–S433.

Anderson R. F., M. P. Bacon and P. G. Brewer (1983a) Removal of Th-230 and Pa-231 from the open ocean. *Earth and Planetary Science Letters*, **62**, 7–23.

Anderson R. F., M. P. Bacon and P. G. Brewer (1983b) Removal of Th-230 and Pa-231 at ocean margins. *Earth and Planetary Science Letters*, **66**, 73–90.

Anderson L. G., E. P. Jones, K. P. Koltermann, P. Schlosser, J. H. Swift and D. W. R. Wallace (1989) The first oceanographic section across the Nansen Basin in the Arctic Ocean. *Deep-Sea Research*, **36**, 475–482.

Bacon M. P. (1988) Tracers of chemical scavenging in the ocean: Boundary effects and large scale chemical fractionation. *Philosophical Transactions of the Royal Society of London, Series A*, **325**, 147–160.

Bacon M. P. and R. F. Anderson (1982) Distribution of thorium isotopes between dissolved and particulate forms in the deep sea. *Journal of Geophysical Research*, **87**, 2045–2056.

Bacon M. P., C.-A. Huh, A. Fleer and W. G. Deuser (1985) Seasonality in the flux of natural radionuclides and plutonium in the deep Sargasso Sea. *Deep-Sea Research*, **32**, 273–286.

Bacon M. P., C.-A. Huh and R. M. Moore (1989) Vertical profiles of some natural radionuclides over the Alpha Ridge, Arctic Ocean. *Earth and Planetary Science Letters*, **95**, 15–22.

Bowen V. T., V. E. Noshkin, H. D. Livingston and H. L. Volchok (1980) Fallout radionuclides in the Pacific Ocean: vertical and horizontal distributions, largely from GEOSECS stations. *Earth and Planetary Science Letters*, **48**, 411–434.

Broecker W. S., A. Kaufman and R. M. Trier (1973) The residence time of thorium in surface sea water and its implications regarding the fate of reactive pollutants. *Earth and Planetary Science Letters*, **20**, 35–44.

Bruland K. W. and K. H. Coale (1986) Surface water Th-234/U-238 disequilibria: Spatial and temporal variations of scavenging rates within the Pacific Ocean. In: *Dynamic Processes in the Chemistry of the Upper Ocean*, J. D. Burton, P. G. Brewer and R. Chesselet, editors, Plenum Publishing Corp., New York, pp. 159–172.

Buesseler K. O., J. K. Cochran, M. P. Bacon, H. D. Livingston, S. A. Casso, D. Hirschberg, M. C. Hartman and A. P. Fleer (1992) Determination of thorium isotopes in seawater by nondestructive and radiochemical procedures. *Deep-Sea Research*, **39**, 1103–1114.

Carpenter R., J. T. Bennett and M. L. Peterson (1981) Pb-210 activities in and fluxes to sediments of the Washington continental slope and shelf. *Geochimica et Cosmochimica Acta*, **45**, 1155–1172.

Casso S. A. and H. D. Livingston (1984) Radiocesium and other nuclides in the Norwegian–Greenland Seas 1981–82. Woods Hole Oceanographic Institution Technical Report, WHOI–84–40, MA, U.S.A.

Coale K. H. and K. W. Bruland (1987) Oceanic stratified euphotic zone as elucidated by Th-234: U-238 disequilibria. *Limnology and Oceanography*, **32**, 189–200.

Cochran J. K., M. P. Bacon, S. Krishnaswami and K. K. Turekian (1983) Po-210 and Pb-210 distributions in the central and eastern Indian Ocean. *Earth and Planetary Science Letters*, **65**, 433–452.

Cochran J. K., H. D. Livingston, D. J. Hirschberg and L. D. Surprenant (1987) Natural and anthropogenic radionuclide distributions in the northwest Atlantic Ocean. *Earth and Planetary Science Letters*, **84**, 135–152.

Cochran J. K., T. Mckibbin-Vaughan, M. M. Dornblaser, D. Hirschberg, H. D. Livingston and K. O. Buessler (1990) ^{210}Pb scavenging in the North Atlantic and North Pacific Oceans. *Earth and Planetary Science Letters*, **97**, 332–352.

Finkel R., S. Krishnaswami and D. L. Clark (1977) Be-10 in Arctic Ocean sediments. *Earth and Planetary Science Letters*, **35**, 199–204.

Fisher N. S., J. K. Cochran, S. Krishnaswami and H. D. Livingston (1988) Predicting the oceanic flux of radionuclides on sinking biogenic debris. *Nature*, **355**, 622–625.

Flynn W. W. (1968) The determination of low levels of polonium-210 in environmental materials. *Analytica Chimica Acta*, **43**, 221–227.

Huh C.-A. and T. M. Beasley (1987) Profiles of dissolved and particulate thorium isotopes in the water column of coastal Southern California. *Earth and Planetary Science Letters*, **85**, 1–10.

Kadko D., M. P. Bacon and A. Hudson (1986) Enhanced scavenging of Pb-210 and Po-210 by processes associated with the East Pacific Rise near 8°45'N. *Earth and Planetary Science Letters*, **81**, 349–357.

Kaufman A., R. M. Trier, W. S. Broecker and H. W. Feely (1973) Distributions of Ra-228 in the world ocean. *Journal of Geophysical Research*, **78**, 8827–8848.

Key R. M., W. S. Moore and J. L. Sarmiento (1992) Transient Tracers in the Ocean: North Atlantic Study — Final Data Report for ^{228}Ra, and ^{226}Ra. Ocean Tracer Laboratory, Princeton University, OTL Technical Report No. 92–2, 193 pp.

Ku T.-L. and W. S. Broecker (1967) Rates of sedimentation in the Arctic Ocean. *Progress in Oceanography*, **4**, 95–104.

Kupferman S. L., H. D. Livingston and V. T. Bowen (1979) A mass balance for Cs-137 and Sr-90 in the North Atlantic Ocean. *Journal of Marine Research*, **37**, 157–199.

Li Y.-H., H. W. Feely and J. R. Toggweiler (1980) Ra-228 and Th-228 concentrations in GEOSECS Atlantic surface waters. *Deep-Sea Research*, **27A**, 545–555.

Livingston H. D. and J. K. Cochran (1987) Determination of transuranic and thorium isotopes in ocean water: In *Solution and in filterable particles. Journal of Radioanalysis and Nuclear Chemistry*, **115**, 299–308.

Livingston H. D., D. R. Mann and V. T. Bowen (1975) Analytical procedures for transuranic elements in seawater and marine sediments. In: *Analytical methods in oceanography*, T.R.P. Gibbs, editor. American Chemical Society, Advances in Chemistry Series, Vol. 147, pp. 124–138.

Livingston H. D., V. T. Bowen and S. L. Kupferman (1982) Radionuclides from Windscale discharges I: Non-equilibrium tracer experiments in high latitude oceanography. *Journal of Marine Research*, **40**, 253–272.

Livingston H. D., S. L. Kupferman, V. T. Bowen and R. M. Moore (1984) Vertical profiles of artificial radionuclide concentrations in the Central Arctic Ocean. *Geochimica et Cosmochimica Acta*, **48**, 2195–2203.

Livingston H. D., J. H. Swift and H. G. Ostlund (1985) Artificial radionuclide tracer supply to the Denmark Strait overflow between 1972 and 1981. *Journal of Geophysical Research*, **90**, 6971–6982.

Mangini A. and R. M. Key (1983) A Th-230 profile in the Atlantic Ocean. *Earth and Planetary Science Letters*, **62**, 377–384.

Moore W. S. (1976) Sampling Ra-228 in the deep ocean. *Deep-Sea Research*, **23**, 647–651.

Moore R. M. and J. N. Smith (1986) Disequilibria between Ra-226, Pb-210 and Po-210 in the Arctic Ocean and the implications for chemical modification of the Pacific water inflow. *Earth and Planetary Science Letters*, **77**, 285–292.

Moore R. M., R. M. Key and J. L. Sarmiento (1985) Techniques for precise mapping of Ra-226 and Ra-228 in the ocean. *Journal of Geophysical Research*, **90**, 6983–6994.

Murnane R. J., J. K. Cochran and J. Sarmiento (1994) Estimates of particle and thorium cycling rate constants in the Northwest Atlantic ocean. *Journal of Geophysical Research*, **99**, 3373–3392.

Nozaki Y., Y. Horibe and H. Tsubota (1981) The water column distributions of thorium isotopes in the western North Pacific. *Earth and Planetary Science Letters*, **54**, 203–216.

Nozaki Y., H.-S. Yang and M. Yamada (1987) Scavenging of thorium in the ocean. *Journal of Geophysical Research*, **92**, 772–778.

Rutgers van der Loeff M., R. M. Key, J. Scholten, D. Bauch and A. Michel (1994) [228]Ra as a tracer for shelf water in the Arctic Ocean. *Deep-Sea Research II*, **42**, 1533–1553.

Schlosser P., G. Bonisch, B. Kromer, K. O. Munnich and K. P. Koltermann (1990) Ventilation rates of the waters in the Nansen Basin of the Arctic Ocean derived from a multitracer approach. *Journal of Geophysical Research*, **95**, 3265–3272.

Scholten J. C., M. M. Rutgers van der Loeff and A. Michel (1994) Distribution of [230]Th and [231]Pa in the water column in relation to the ventilation of the deep Arctic basins. *Deep-Sea Research*, **42**, 1519–1531.

Shimmield G. B. and N. B. Price (1988) The scavenging of U, Th-230 and Pu-231 during pulsed hydrothermal activity at 20°S, East Pacific Rise. *Geochimica et Cosmochimica Acta*, **52**, 669–677.

Thiede J. (1988) Scientific Cruise Report of Arctic Expedition ARK IV/3. Reports on Polar Research 43, Alfred-Wegener Institute fur Polar-und Meeresforschung, 237 pp.

Wallace D. W. R. and R. M Moore (1985) Vertical profiles of CCl_2–CF_2 (F-12) and CCl3F (F-11) in the Central Arctic Ocean Basin. *Journal of Geophysical Research*, **90**, 1155–1166.

Wallace D. W. R., P. Schlosser, M. Krysell and G. Bonish (1992) Halocarbon ratio and tritium/[3]He dating of water masses in the Nansen Basin, Arctic Ocean. *Deep-Sea Research*, **39**, S435–S458.